Iranian Journal of Chemical Engineering
Vol. 6, No. 3 (Summer), 2009, IAChE

Effects of Vertical Temperature Gradient on Heavy Gas Dispersion in Build up Area

E. Kashi[1], F. Shahraki[2], D. Rashtchian[3], A. Behzadmehr[4]*

1,2- Department of Chemical Engineering, University of Sistan and Baluchestan, Zahedan, Iran.
3- Department of Chemical and Petroleum Engineering, Sharif University of Technology, Tehran, Iran.
4- Department of Mechanical Engineering, University of Sistan and Baluchestan, Zahedan, Iran.

Abstract

Dispersion of heavy gases is considered to be more hazardous than the passive ones because it takes place more slowly. When the gas is accidentally released at ground level or where there are many obstacles in the area it is considered to be a heavy gas. In this paper, based on the extensive experimental work of McQuid and Hanna, the model was tested against two types of experiments: A simple experiment "Thorney Island" and a complex experiment "Kit Fox" in order to validate CFD code. In order to accomplish this validation the multiphase approach was employed. Also, the vertical temperature gradient in the atmosphere was investigated. The investigation of wind speed was done taking factors such as time, height and direction into consideration. In order to reduce the number of elements in the computational domain, a combination of 2D and 3D geometry was utilized. The results showed that the wind inlet correction, as well as the temperature gradient, had a significant influence on gas concentration records.

Keywords: *Heavy gas dispersion, Temperature gradient, Complex train, CFD*

1- Introduction

In today's modern industry, large quantities of hazardous toxic substances are produced, stored or transported. Many of these substances are gases that form clouds heavier than air when accidentally released into the atmosphere. These gases may have a density greater than that of the air for several reasons including the high molecular weight (like chlorine), low release temperature (like liquefied natural gas), high storage pressure (for example a failure of the container of ammonia and subsequent formation of aerosol) or chemical reactions of the released substances with water vapor in the atmosphere (the polymerization of hydrogen fluoride) [1].

The heavy gas cloud has the negative

* Corresponding author: fshahraki@hamoon.usb.ac.ir

buoyancy that affects and modifies its behavior when compared to a positively or neutrally buoyant cloud. These effects include the additional gravity driven flow, wind shear at the heavy gas cloud interfaces, turbulence dumping, and inertia of the released material. Some special models have been developed to describe the heavy gas clouds dispersion in the atmospheric air known as heavy gas dispersion models or dense gas dispersion models [2].

These models include empirical, intermediate and fluid dynamic models. The empirical and intermediate models are important components of emergency response systems and valuable tools for environmental impact assessment and risk assessment. The fluid dynamics models are usually used as a research tool to better understand the properties of the heavy gas.

Computational fluid dynamics allows the simulation of complex physical processes describing heat and mass transport phenomena with fully developed mathematical models. Specific models incorporated in CFD codes predict the turbulent mixing between gas molecules and air particles. This mostly happens in cavity regions in the flow field (building wakes), which may result in the entrapment of escaping gas at low heights for relatively long periods of time with increased health effects [3].

Dense gas dispersion modeling in the obstacle area, because of sensitivity to various parameters and conditions, is very complicated and is an interest in many researches, both in safety and environmental fields. Some of the recent CFD works on gas dispersion modeling have focused on obstacle effects on gas concentration phenomena [4-9], while others studied the effects of heat transfer on LNG spills [10-12]. In this paper, numerical simulation of the Thorney Island trials and Kit Fox field experiments were performed using ANSYS CFX 11 code [13]. In this paper, CFD code is used to investigate some of the essential parameters in dense gas dispersion modeling (e.g. obstacle effects, wind profile, atmospheric stability and CFD parameters like mesh type and size, turbulence models, various boundary conditions) in the obstacle area.

The special studies which have been taken in to consideration in this paper are:

a) Using and testing multiphase approach instead of the additional variable model and multicomponent model for dense gas dispersion modeling.
b) A new method for wind inlet at the inlet boundary condition is used, which is three dimensional and time-dependent wind speed, instead of the usual wind profile, and is included in the model.
c) A buoyancy model (Boussinesq), instead of atmospheric stability models, is used and its effects have been studied.
d) Hybrid 2D and 3D geometry is used in order to reduce the number of meshes and computational time.

2- Field experiments

Although the primary benefit of the application of CFD methods is to simulate the flow around obstacles, it is important to demonstrate the ability of the CFD code to correctly model gas dispersion in the absence

of complex buildings where the flow is relatively simple and well-defined. By using this procedure any problems within the code, can be more easily identified and resolved. So, at first, the Thorney Island experiment has been simulated as a simple case and then the Kit Fox experiment is considered as a more complex experiment. Field gas dispersion experiments are very expensive and set up in some large projects, so it is not the aim of this work and, consequently, we had to use standard experiments by permission.

2.1. Thorney island experiment

The Thorney Island Heavy Gas Dispersion Trials were organized by the Health & Safety Executive and their related detailed information has been given by McQuaid and Roebuck [14]. This experiment was investigated by Hall [15] and Sklavounos and Rigas [3]. Fig. 1 shows the schematic of trial no. 26 of phase two which is considered in this simulation.

2.2. Kit Fox field experiment

A joint field experiment (named "Kit Fox") was conducted in August and September, 1995, at the Frenchman Flat area of the Nevada Test Site (NTS). The field operations, described in the WRI report [16], were carried out by Western Research Institute (WRI) and Desert Research Institute (DRI). There were 52 independent Kit Fox data trials, with about 2/3 for “puff” or ”finite duration” 20s releases, and about 1/3 for “continuous plume” 120-450s releases. A summary of the major characteristics of each of the 52 tests is given by Hanna and Chang [17, 18]. Fig. 2 shows the plot plan of the Kit Fox experiment. In this paper trial 3-7 (trial 3, release 7; an instantaneous release) are implemented for simulation purposes.

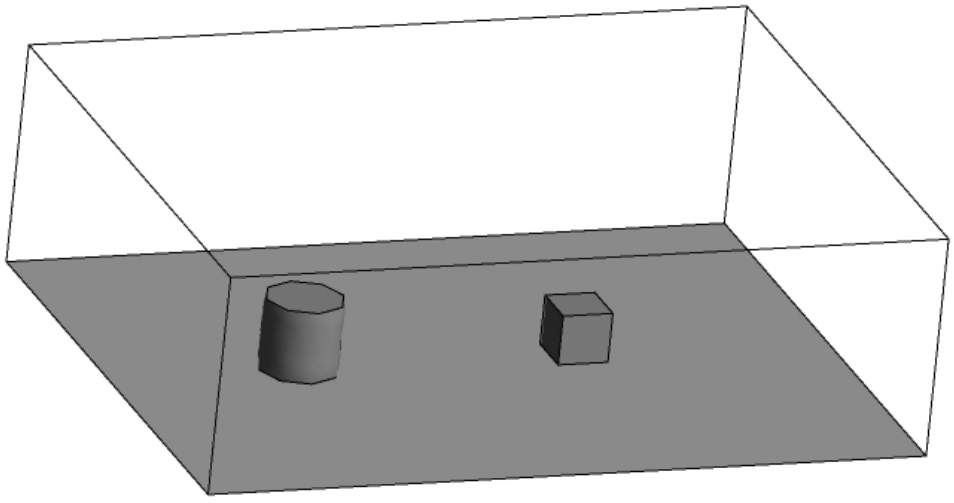

Figure 1. Schematic of trial no. 26 from Thorney Island experiment

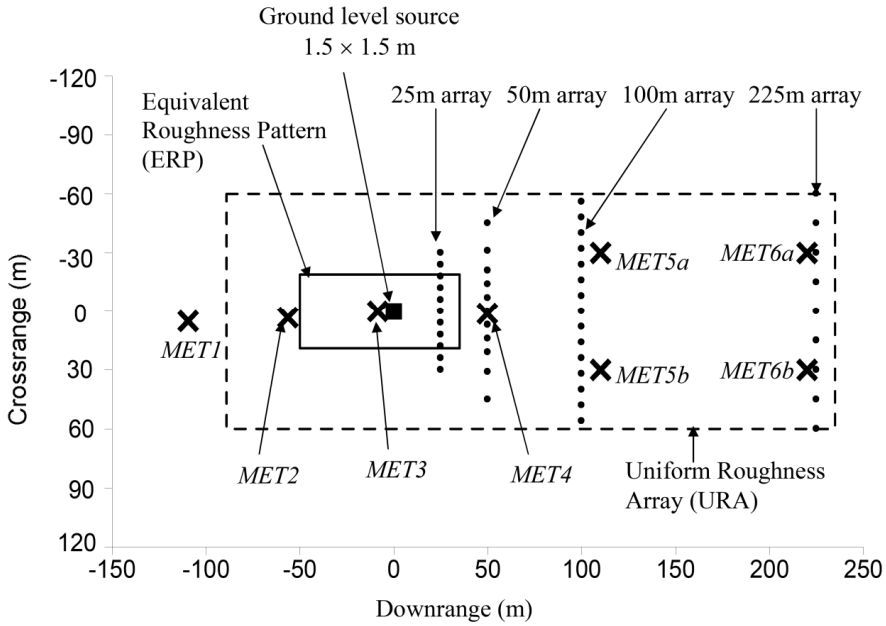

Figure 2. Plot plan of the Kit Fox dispersion grid including meteorological towers, concentration monitoring arcs, gas source, Equivalent Roughness Pattern (ERP), and Uniform Roughness Array (URA).

3. Mathematical formulation

Gas dispersion in atmosphere can be studied in different methods using CFD code. These methods include studying a flow with an additional variable, a flow with multi-component fluid and a multiphase flow. Using additional variables can help in modeling the transport of a passive material in the fluid flow like smoke in the air. The presence of an additional variable does not affect the fluid flow, even though some fluid properties may be defined to be dependent on additional variables. In multicomponent flow method it is assumed that different components of a fluid are mixed together at molecular level sharing the same mean velocity, pressure and temperature fields. Also, in this approach mass transfer is considered to take place by convection and diffusion. In more complex situations where different components are mixed on larger scales and with separate velocity and temperature fields, multiphase flow method is used.

In this paper, in order to model dense gas dispersion the multiphase flow method was employed. ANSYS CFX was used as a computational code for simulation purposes. In ANSYS CFX the equations of momentum, mass transfer, heat transfer, buoyancy and the turbulence model for homogeneous multiphase flow are supposed to be solved using the finite volume method.

4. Simulations and results

4.1. Thorney island case

ANSYS Workbench Design Modeler and CFX-Mesh tools were used for creating and

meshing geometry. Using embedded meshing techniques, cells are concentrated around the initial position of the gas cloud in order to capture the detailed shear and entrainment effects at the edge of the gas column. In addition, a fine resolution was used vertically from the ground up to a height of about 2m. In this case 10 inflation layers were used with a first layer thickness of 0.01m. Cells close to the cube were also concentrated to help resolve the interaction problems between the cloud and obstacle. Maximum distance of meshes near the initial gas cloud is 0.5m and the normal maximum distance is 2m.

Computational grids consist of 331179 cells. Since the purpose of the study was to compute concentration values in time, the problem was solved in transient form. Total simulation time was 200s with relatively short time steps (1s). The convergence criterion was the RMS (residual of root mean square) that was considered to be equal to or less than 10^{-4}. Transient runs needed 3–8 iterations per time step to reach the desirable residual value.

In order to reduce the number of meshes and then decrease the computing time a symmetry plane was used. The model geometry is shown in Fig. 3. The extent of the domain was 130m in the x-direction, 100m in the y-direction and 40m in the z-direction.

As mentioned earlier, R-12 and Nitrogen were used in the Thorney Island experiment. Therefore these two gases are considered in addition to air in the domain. Since Thorney Island trials were conducted at a neutral atmospheric condition and temperature data are not available we do not consider heat transfer models, and actually the equation of energy is not taken into account. Assuming there might be turbulence in the domain the standard k-ε model was used.

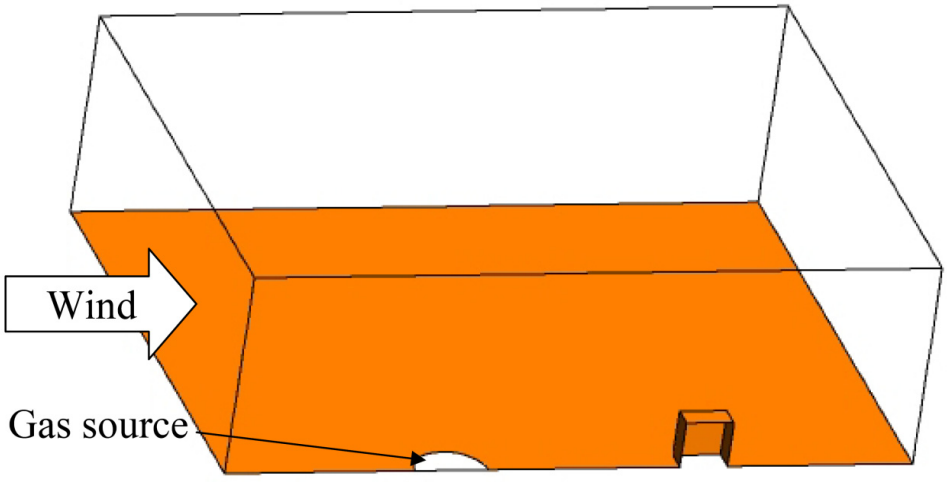

Figure 3. Domain of simulation in Thorney Island experiment (half of the main domain)

4.1.1. Boundary conditions

Taking into consideration the computational domains shown in Fig. 3, the boundary conditions set for the wind profile and gas inflow are demonstrated below.

4.1.1.1. Gas inlet

Approximately 2000m^3 of Freon 12/nitrogen mixture was released into the atmosphere instantaneously at Thorney Island no. 26. In order to set the inflow boundary condition for the transient problem, released mixture mass inflow rate (Q_i) was given through a properly adapted step function:

$$Q_i = m_i \times step\left[-\frac{(t-t_0)(t-t_1)}{t_0^2}\right] \quad (1)$$

where m_i is equal to 4780 kg s^{-1}.

The gas was released from the ground level source to the domain for 1s, elevating to a 13m height. After 1s a cylindrical cloud was formed. This condition was the same as the experimental condition and positively affected the simulation process.

4.1.1.2. Wind inlet

Wind speed is one of the most significant parameters in the problem definition procedure, since it determines how quickly emitted gas will be diluted by passing volumes of air. The corresponding boundary condition should take into account the reduction of wind speed value near the ground level due to the frictional effects. If wind speed at a fixed height is known (typical reference height 10m), then the wind velocity profile may be given through a power low correlation [19]:

$$u_z = u_0 \times \left(\frac{Z}{Z_0}\right)^{\lambda} \quad (2)$$

where λ is a dimensionless parameter whose value depends upon the atmospheric stability category and surface roughness (Z_0). Regarding the trial 26, the value of Z_0 is 0.005m; λ is 0.07and u_0 is 1.9m/s.

In addition to the above mentioned boundary conditions, the ground and the building surfaces were defined as fixed stable walls, where according to the no-slip condition the fluid velocity is equal to zero. As mentioned earlier, half of the domain is considered because of symmetry, while the remaining surfaces of the domain were specified via a relative pressure value that was set equal to zero (opening condition).

4.1.2. Results

In Fig. 4 the predicted concentration is compared with the experimental concentration measured on the front face of the building at the height of 6.4m. These results show that this model can be used for the Kit Fox experiment (as a complex experiment). It is seen that the simulation results are in good agreement with the experimental data and it can be hoped that good results from the simulation of the complex experiment will be seen.

4.2. Kit Fox case

Like in the Thorney Island case, ANSYS workbench Design modeler and CFX mesh tools were used for making the geometry of the domain and meshing it. In this simulation, two-dimensional boards were used as ERP obstacles. In this way the

thickness of the obstacles is eliminated and as a result even the smallest mesh can be greater than the billboard thickness. The model geometry is shown in Fig. 5.

Using line control techniques, cells were concentrated around the obstacles area. Also, a fine resolution was implemented vertically from the ground up to a height of about 1m. In this study 20 inflation layers were used. The thickness of the first layer was determined at the beginning. Since the CFX code used the wall function in its simulation and the near wall meshes are very important, the determination of the first layer was done using y^+ means. This can help attain the best results from the CFD code. Maximum distance of meshes in the area around the obstacles is 0.5m and the normal maximum distance is 2m. Fig. 6 shows the refinement of meshes near the surface and around the obstacles. The fine meshes covered a volume of 6*50*100m (height*latitude* longitude)

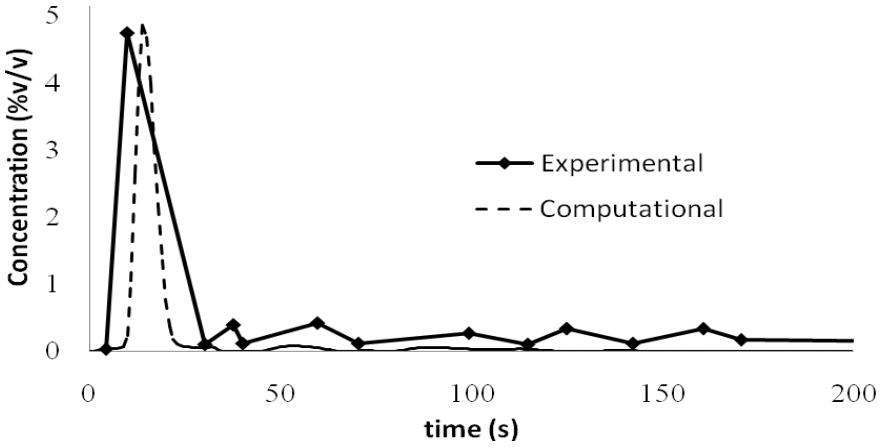

Figure 4. Gas concentration vs. time for Thorney Island experiment (trial no. 26), front face of the building at height 6.4m.

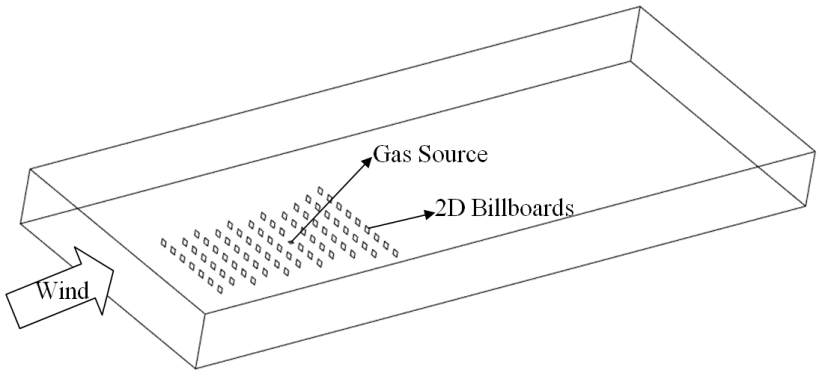

Figure 5. Domain of simulation of Kit Fox experiment

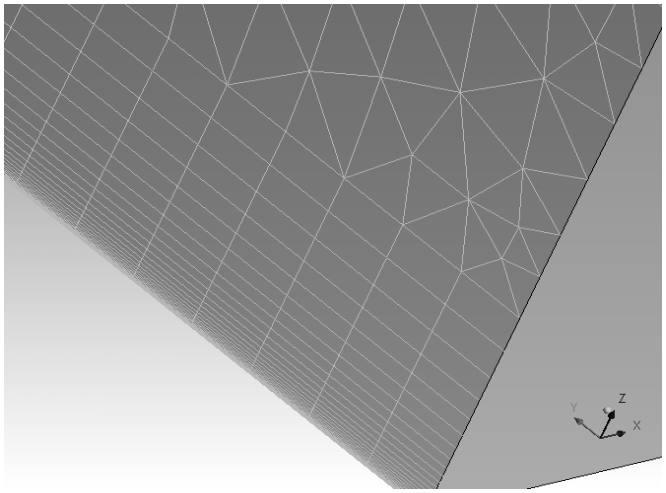

Figure 6. Surface mesh of trial 3-7 from Kit Fox experiments

Computational grids consist of 1716184 cells. The problem was solved in transient form. Total time for simulation was set to be 250s with relatively short time steps (0.25s). The following hypotheses are considered. The fluid under consideration is a mixture of air and CO_2. The air temperature was not fixed and it varied vertically (in Z direction, see Fig. 7). Therefore the computation was carried out using thermal energy, and because of the low temperature gradient, the Boussinesq buoyancy model was used. Since the flow was assumed to be turbulent the standard k-ε model was used.

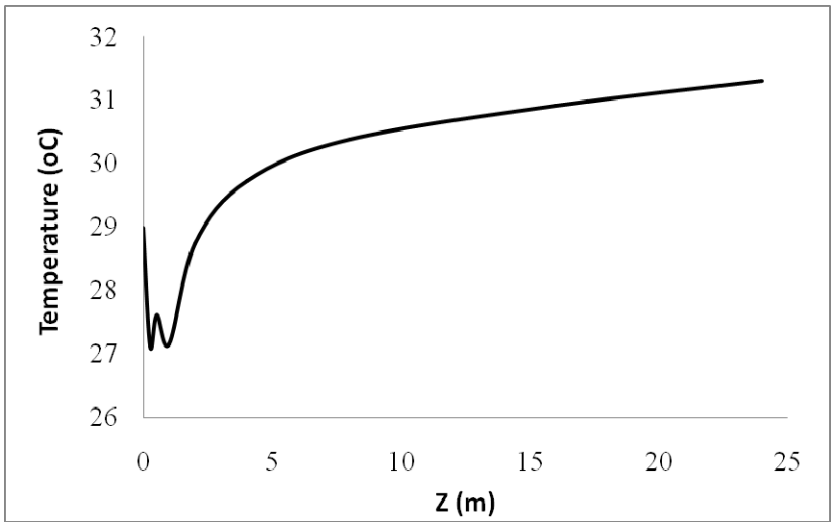

Figure 7. Vertical temperature gradient in the EPA tower location

4.2.1. Boundary conditions

4.2.1.1. Gas inlet

In trial 3-7 of the Kit Fox field experiment, carbon dioxide was released instantaneously into the atmosphere with a 3.65kg/s rate and for about 20s. In order to set the inflow boundary condition, as in the Thorney Island case, the mass inflow rate of the gas from the surface level was specified (m_i=3.65kg/s, t_l=50s). In order to have a fully developed flow in the domain, the gas was released after 50s. Since the gas was released at the ground level and during the experiment the ground surface temperature was 29°C, the gas temperature was set to be 29°C in the simulation.

4.2.1.2. Wind inlet

When there is low wind speed condition, wind direction can vary considerably within small periods of time. Low wind speeds are associated with a phenomenon called meander which is a horizontal oscillation of the local atmosphere. As the wind velocity decreases below a certain threshold, it is no longer possible to define a mean wind direction (see Fig. 8). These oscillations are independent of atmospheric stability or topography and are related to the equilibrium between the coriolis force and the pressure gradient [20]. Accordingly, in order to get better results there was no use of correlation in this simulation. The EPA tower wind data (see section 3.2) was directly used as the wind inlet boundary condition. This procedure can be useful in defining the wind speed and its direction any time and in any height. The average values of wind speed and its direction are given in Table 1. Cartesian velocity component was used for adding wind direction:

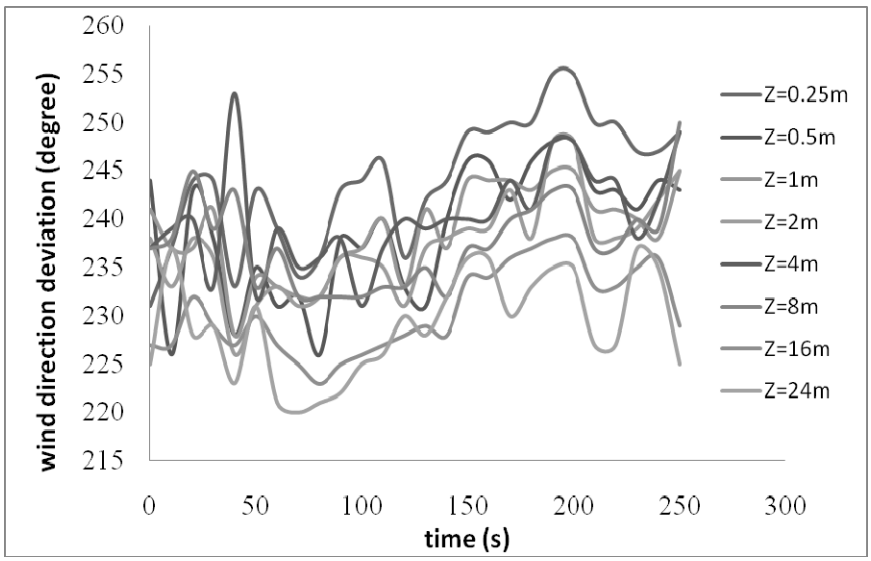

Figure 8. Wind direction deviation with time at the EPA tower

Table 1. Wind speed and direction deviation with time and height in EPA tower, in trial 3-7 of Kit Fox experiments

	Wind speed (m/s)								Wind direction (deg.)							
Time	**Z=0.25**	**0.5**	**1**	**2**	**4**	**8**	**16**	**24**	**0.25**	**0.5**	**1**	**2**	**4**	**8**	**16**	**24**
19:27:20	1.39	1.51	1.99	2.47	2.94	3.39	4.2	5.47	234	233	231	229	228	231	228	228
19:27:30	1.39	1.51	1.99	2.47	2.83	3.19	4.2	4.82	239	236	235	230	232	235	233	231
19:27:40	1.39	1.51	1.99	2.47	2.83	3.19	4.2	4.82	239	236	235	230	232	235	233	231
19:27:50	1.39	1.51	1.89	2.47	2.83	3.19	4.38	5.77	240	236	235	231	233	234	240	226
19:28:00	1.51	1.51	1.89	2.37	2.83	3.19	4.16	5.45	243	238	237	235	235	236	232	223
19:28:10	1.51	1.69	2.07	2.37	2.83	3.19	4.16	5.23	242	236	238	235	238	239	232	233
19:28:20	1.51	1.69	2.07	2.37	2.83	3.19	4.16	5.23	242	236	238	235	238	239	232	233
19:28:30	1.63	2.09	2.58	3.21	3.47	3.96	4.53	5.01	231	244	241	238	237	237	227	225
19:28:40	2.3	2.74	2.97	3.21	3.01	3.6	4.53	5.27	237	226	237	233	239	238	227	237
19:28:50	1.65	1.99	2.3	2.64	3.01	3.6	4.53	5.54	244	243	237	238	240	245	232	228
19:29:00	1.65	1.99	2.3	2.51	2.87	3.6	4.53	5.64	244	238	241	236	233	239	229	229
19:29:10	1.49	1.71	1.94	2.51	3.01	3.72	4.4	5.49	233	228	228	226	253	243	227	223
19:29:20	1.87	1.86	2.18	2.51	2.74	3.19	4.4	5.22	243	235	234	231	232	233	230	231
19:29:30	1.49	1.73	2.01	2.37	2.88	3.6	4.27	5.22	239	231	233	233	239	237	227	221
19:29:40	1.63	1.73	2.01	2.61	2.88	3.48	4.49	5.22	234	232	232	231	235	232	225	220
19:29:50	1.63	1.73	2.01	2.49	2.74	3.36	4.36	5.22	236	226	232	232	236	232	223	221
19:30:00	1.51	1.73	2.01	2.49	2.88	3.36	4.13	5.1	243	238	236	236	238	232	225	222
19:30:10	1.51	1.73	2.01	2.49	2.88	3.21	4.13	5.1	244	237	237	236	231	232	226	225
19:30:20	1.89	1.85	2.01	2.35	2.88	3.65	4.29	5.1	246	240	240	235	237	233	227	226
19:30:30	1.89	2.21	2.41	2.56	2.88	3.65	4.29	4.9	236	233	233	231	240	233	228	230
19:30:40	1.77	1.68	2.08	2.56	3.03	3.65	4.53	5.1	242	231	241	237	239	235	229	228
19:30:50	1.89	1.97	2.08	2.56	3.03	3.76	4.34	4.86	244	240	237	238	240	232	228	232
19:31:00	1.68	1.97	2.22	2.56	3.03	3.5	4.53	5.1	249	246	244	239	240	237	234	236
19:31:10	1.68	1.97	2.22	2.56	3.03	3.5	4.53	5.1	249	246	244	239	240	237	234	236
19:31:20	1.68	1.86	2.22	2.56	3.03	3.5	4.38	5.1	250	242	244	243	244	240	236	230
19:31:30	1.53	1.86	2.22	2.56	3.03	3.5	4.24	5.1	250	246	243	238	241	241	237	233
19:31:40	1.68	1.86	2.22	2.56	3.14	3.69	4.44	4.75	255	248	245	248	248	243	238	235
19:31:50	1.68	1.86	2.22	2.56	3.14	3.69	4.44	4.75	255	248	245	248	248	243	238	235
19:32:00	1.68	1.86	2.22	2.77	3.39	3.69	4.44	5.18	250	243	241	238	244	237	233	227
19:32:10	1.68	1.86	2.22	2.77	3.39	3.69	4.44	5.18	250	243	241	238	244	237	233	227
19:32:20	1.53	1.86	2.22	2.63	3.12	3.69	4.44	4.94	247	241	240	239	238	240	235	237
19:32:30	1.53	1.86	2.22	2.63	3.12	3.43	4.29	4.94	247	244	238	242	242	239	236	235
19:32:40	1.53	1.75	2.22	2.63	3.12	3.63	4.09	4.2	249	243	245	245	249	250	229	225

$$u = U\cos\theta \quad (3)$$

$$v = U\sin\theta \quad (4)$$

$$w = 0 \quad (5)$$

where θ is a deviation of wind direction. To consider the time variation of the wind speed and its direction in time, in the simulation step function. In this way, in comparison to the existing wind profiles like the logarithmic profile, the wind velocity was more accurately modeled (see Figs. 9 and 10). Also, there is no need to extend the longitude and altitude of the simulation domain. Figs. 9 and 10 show wind speed dependency on time and height at x direction. Since in this trial the normal wind direction has deviations from normal *x* line, both the front and right sides of the domain were defined as the wind inlets. *u* component at the front side and the *v* component at the right side were dominant.

Temperature gradient data were used as the heat transfer boundary condition for all vertical boundary surfaces. Figure 7 shows the vertical temperature gradient in the domain.

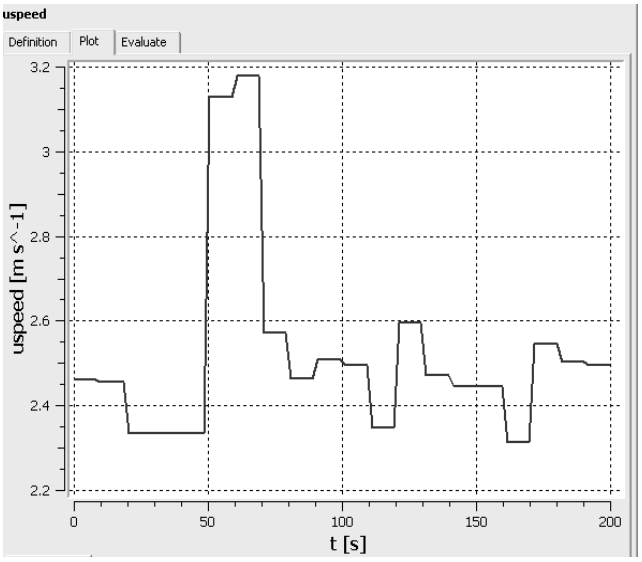

Figure 9. u component of wind speed at the height of 2m in EPA tower location that was included in the simulation

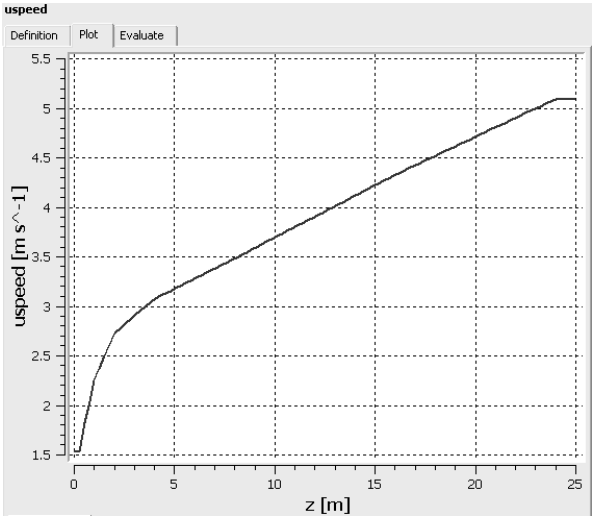

Figure 10. u component of wind speed from 10 to 20 seconds after gas release in EPA tower location that was included in the simulation

4.2.1.3. Surface roughness

The surface roughness length, Z_o, is a measure of the amount of mechanical mixing introduced by the surface roughness elements. The appropriate wind profile formula for nearly neutral conditions is:

$$\frac{u}{u^*} = \frac{1}{\kappa}\ln\left(\frac{Z}{Z_0}\right) \tag{6}$$

where κ is the von Karman constant (assumed to be equal to 0.4) and u^* is the friction velocity. Z_0 can be obtained from these relations [21]:

$$Z_0 = \beta \frac{\nu}{u^*} \tag{7}$$

$$\ln \beta = \ln \frac{eu^*}{\nu} - 3.4 \tag{8}$$

where e is the real roughness height, and ν is the kinematic viscosity. As a rough rule of thumb, Z_0 is equal to about 0.1 times the average height of the roughness elements [22]. In this simulation the ground surface was defined as a rough wall with Z_0 equal to 0.01m.

As mentioned earlier, the ground surface temperature was 29°C at the time of the experiment. Therefore the surface temperature was set to be 29°C.

4.2.2. Results and discussion

Since the average velocity of air before gas release is 2.7m/s and the distance between the front surface of the domain (wind boundary condition) and gas source is about 90m, the air particles need at least 50 seconds to reach the source. For the simulation, since the gas was discharged from the source 50s after introducing the air into the domain, the velocity values of the air were taken into consideration 50s before the gas release. This helped maximize the effects of wind speed variations on gas dispersion in the domain.

In order to investigate the grid performance, the problem was solved in a steady state condition. Flow vectors were studied on different planes. Figs. 11 and 12 show the wakes that were produced at the rear of the obstacles. As expected there is a flow recycle in these areas. After releasing the gas and its dispersion, there was a large amount of gas for a long time at the rear of the obstacles and this formed some new sources. Since the ground surface temperature was 29°C during the experiment (Table 1) and while the adjacent air temperature was about 27°C, air got warm near the surface and moved upward. Since the upper limit of the calculation domain had a temperature of 31.4°C, the warmed air cannot move upward and is forced to go down to the surface. This results in buoyancy turbulence production and causes the gas to disperse with a more complex behavior. This phenomenon is shown in Fig. 13. As shown, this phenomenon does not exist in the free obstacle areas. In fact, the flow has little time to warm and goes up in this area; however there is plenty of time for the flow to be warm with the surface heat flux and moves upward in obstacle areas. This is a naturally expected important phenomenon that was ignored in the earlier CFD simulations of gas dispersion. Fig. 13 also shows that the array of obstacles can easily change the flow direction. This figure shows different velocity vector directions inside and outside the obstacled area. This atmospheric condition happens in the afternoons because the earth is usually warmed by solar energy at noon and is still warm, so it exchanges its heat with the adjacent air that is cooler now. This phenomenon can cause faster dispersion of gas, however the prediction of gas concentration may become somehow difficult.

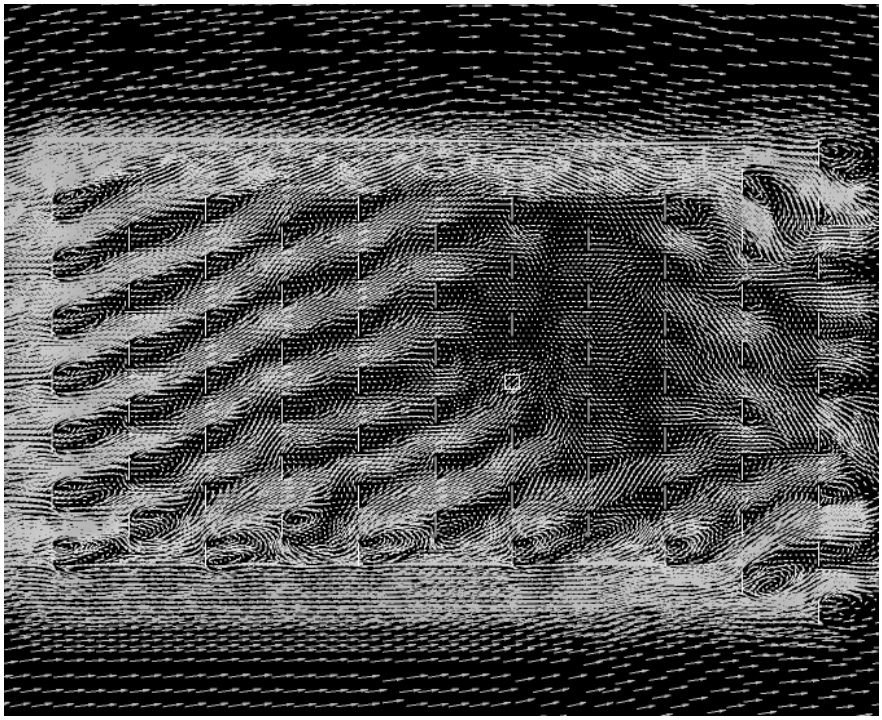

Figure 11. Flow vectors on the 1m elevated plane

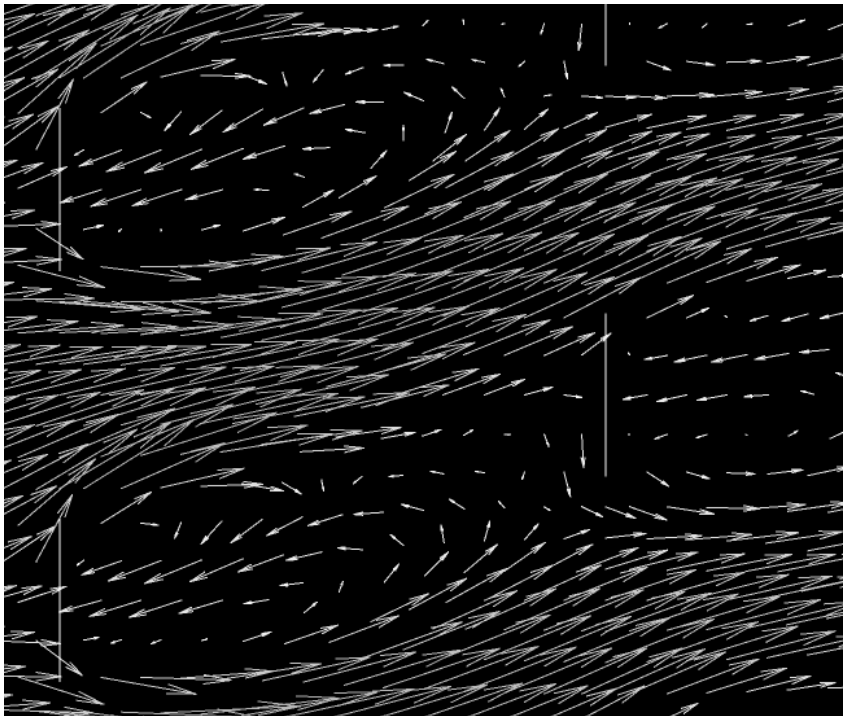

Figure 12. Flow vectors rear of obstacles on the horizontal plane at 1m elevation

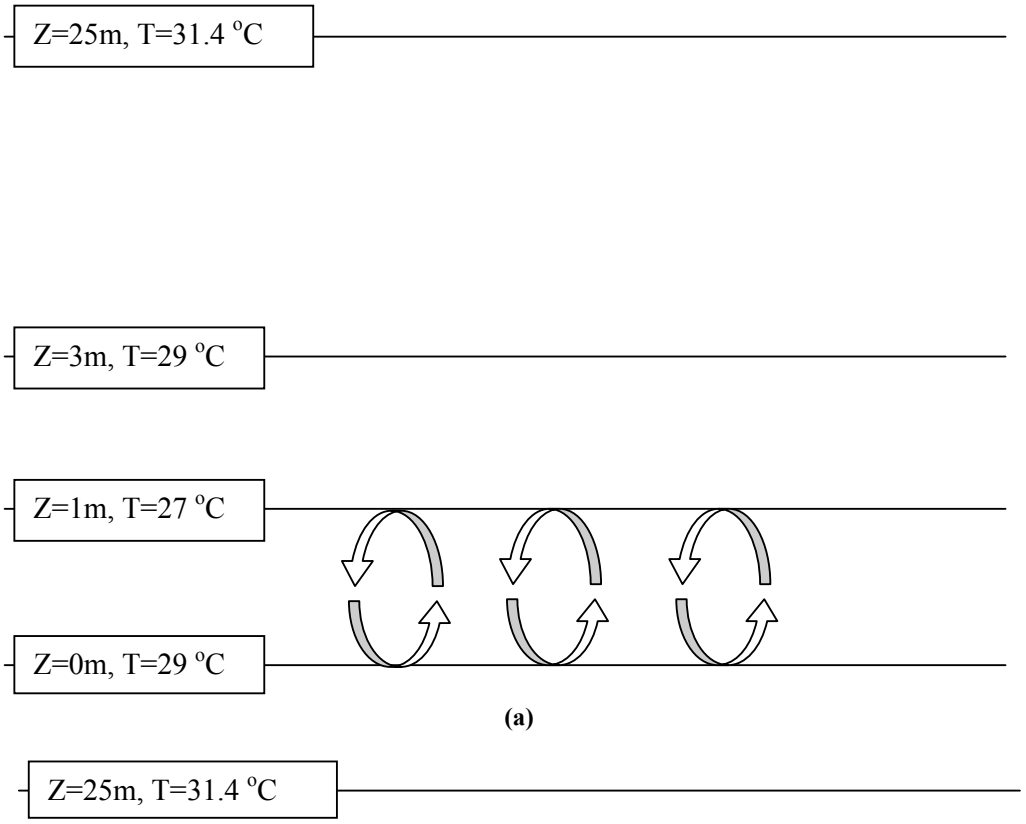

Figure 13. Flow recycles in the obstacle area

For comparison purposes this simulation was also carried out with logarithmic wind profile (without heat transfer model). In Figs. 14-17 gas concentration histories were compared taking the presence and absence of the heat transfer model and logarithmic wind profile conditions into consideration with the values recorded on arc one (25m far from the source) at heights of 0.3m, 0.6m, 1.2m and arc two (50m far from the source) at the height of 0.5m. Unfortunately, as these figures show, the concentration histories are better matched with the experimental results when the heat transfer model is excluded. When the heat transfer model is included, the vertical fluctuation is produced in the flow pattern and consequently the gas dispersion is more complex and its concentration does not match very well with the experimental results.

Comparing the vertical velocity component that is produced by heat transfer between the surface and adjacent air in cases with and without the heat transfer model (Fig.18), we can see that in the second case vertical velocity does not exist, and therefore, if we eliminate the heat transfer model, actually this vertical velocity will be eliminated and gas dispersion is carried out in z direction only by molecular diffusion. This figure also shows the negative speed of the flow in the z direction near the surface. These findings illustrate the advantages of using heat transfer model.

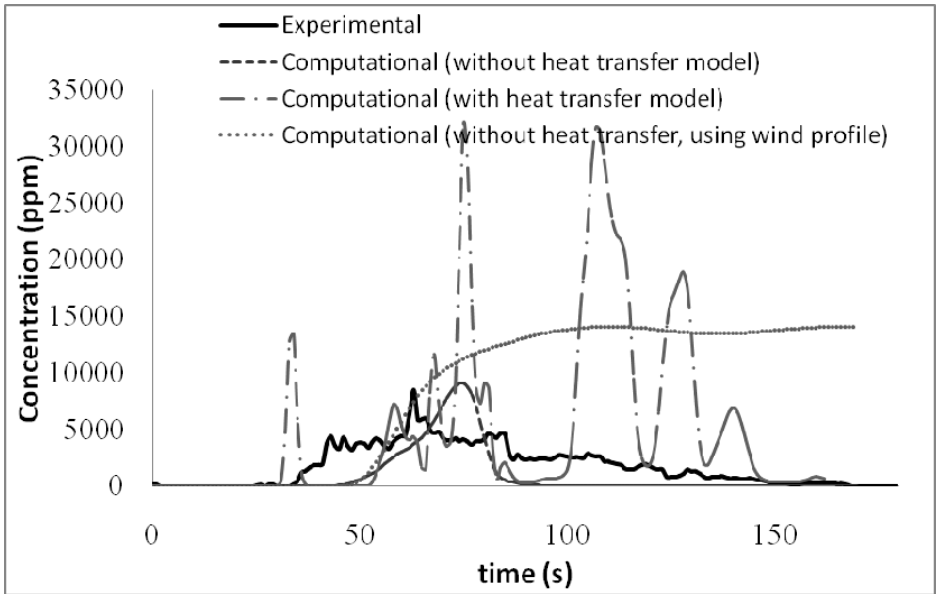

Figure 14. Comparison of experimental and computational results in Kit Fox experiment (trial 3-7) on arc one, at height 0.3m.

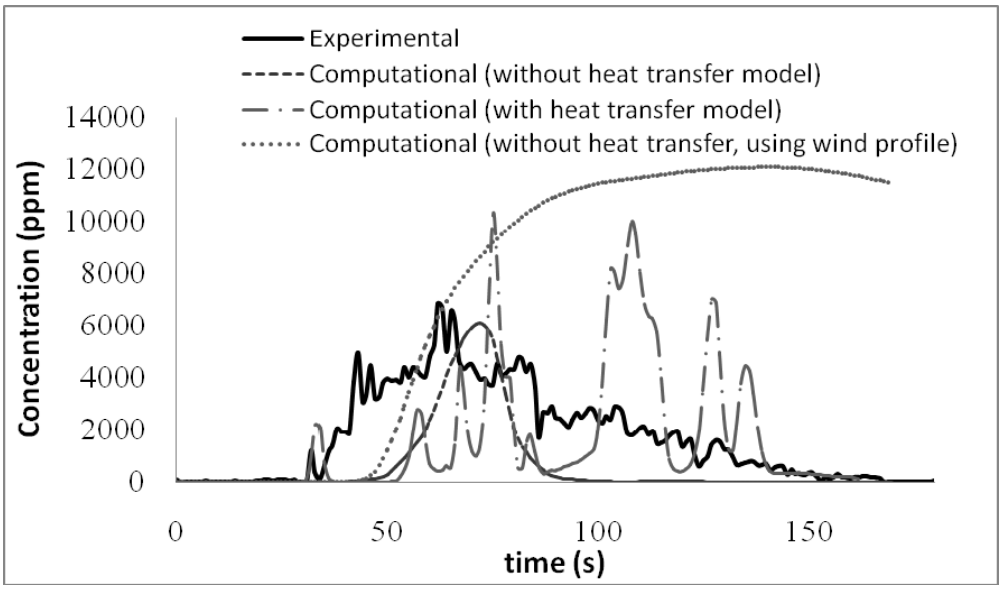

Figure 15. Comparison of experimental and computational results in Kit Fox experiment (trial 3-7) on arc one, at height 0.6m.

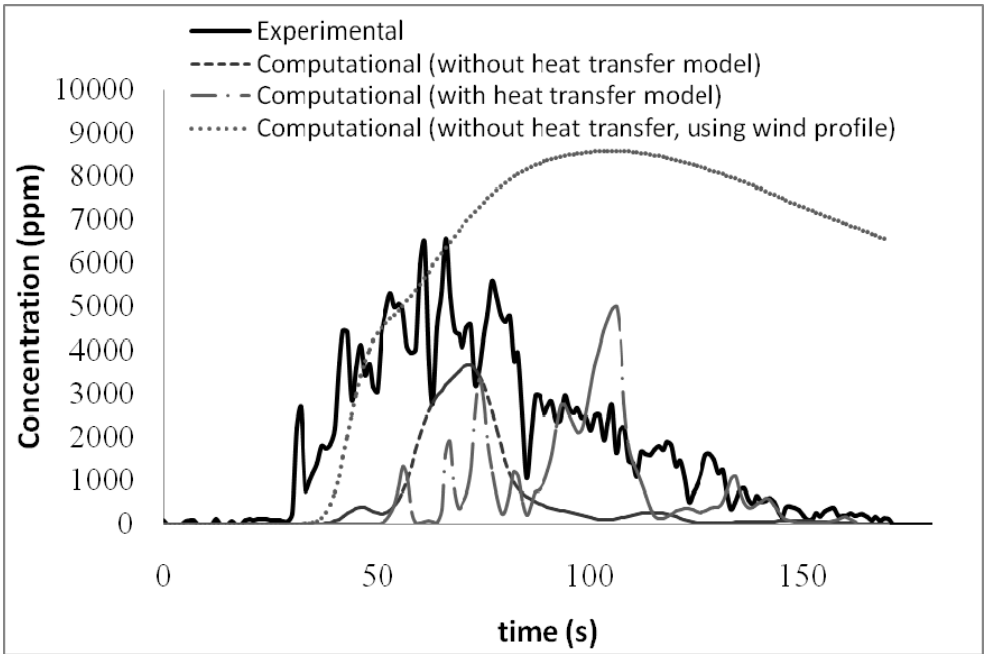

Figure 16. Comparison of experimental and computational results in Kit Fox experiment (trial 3-7) on arc one, at height 1.2m.

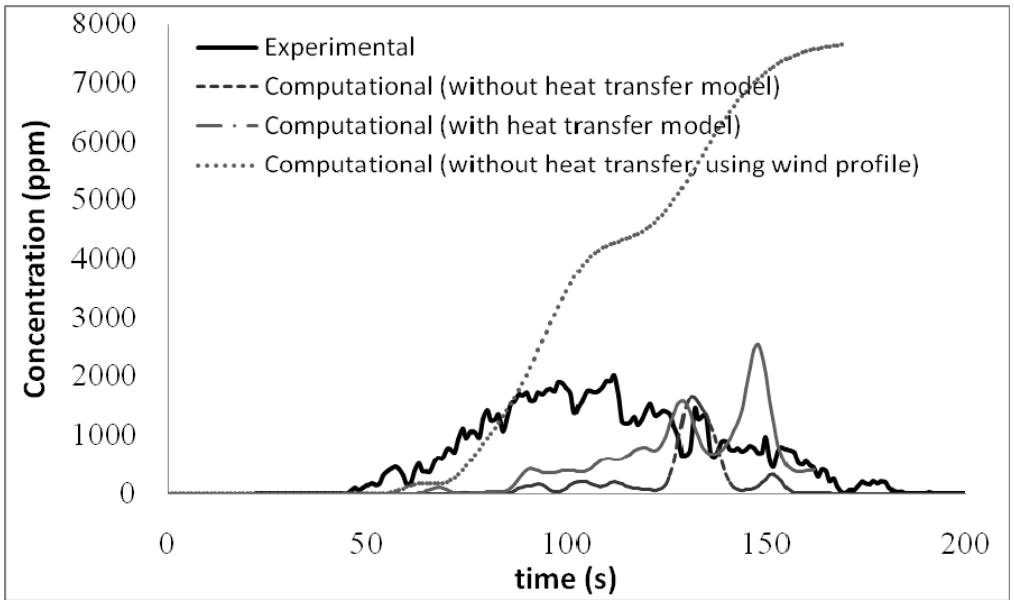

Figure 17. Comparison of experimental and computational results in Kit Fox experiment (trial 3-7) on arc two, at height 0.5m.

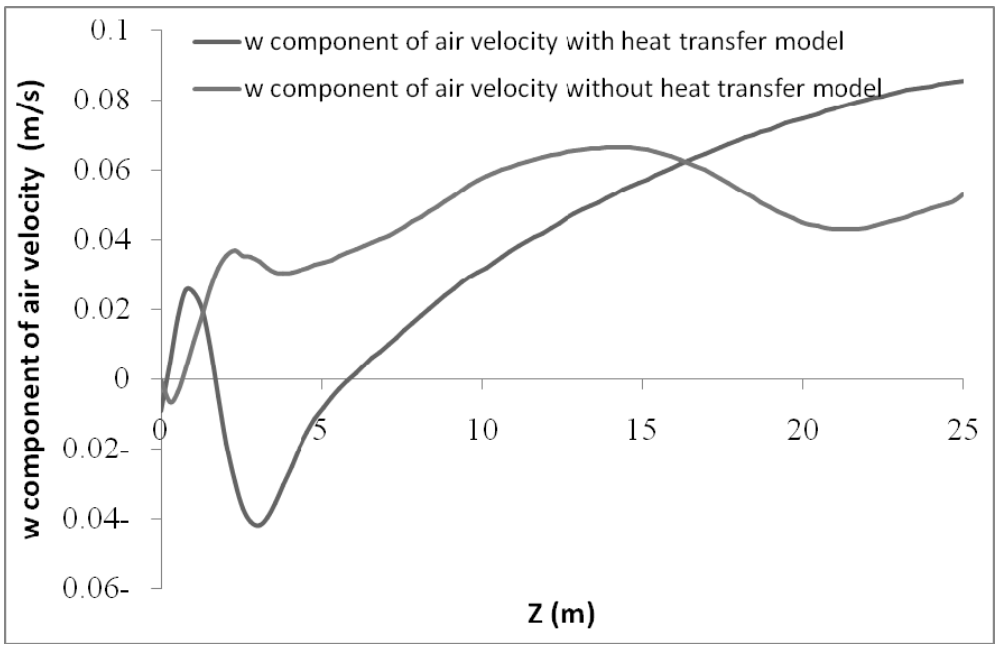

Figure 18. Comparison of w component of air velocity in z direction at 25m far from source point

When the dense gas is released, contrary to the passive gas, it moves upward and flows like a liquid. This phenomenon is clearly shown in Fig. 19. Once the dispersion of the gas is over the gases obstructed at the rear of the obstacles act like secondary sources and therefore the gas dispersion process will continue for longer periods of time. Contrary to the old gas dispersion models, the CFD models can properly show this phenomenon.
CFD postprocessor also can help figure out the volumes of clouds of the flammable gases that have concentrations higher than their related LFL. The weight of the gas cloud can also be obtained. This can be used for calculating the power of an explosion.

5- Conclusion

Computational simulations of atmospheric dispersion of gas around both an isolated cubical obstacle and an array of obstacles were conducted using the code CFX11. The model was validated using the results of Thorney Island and Kit Fox experiments. The fluctuations of wind speed and its direction are the most important factors in an accidental gas release. By including experimental wind speed and direction data at different times and elevations in CFD code, the concentration results can be predicted more carefully. In addition, the near wall mesh size is an important parameter that can affect gas dispersion. Using y^+ means at the mesh generation stage helped in achieving acceptable and desirable results more easily. The vertical temperature gradient is an important phenomenon in gas dispersion modeling that has been shown by stability class in old models. In CFD models, temperature gradient should be considered in the simulation as a boundary condition using profiles or raw experimental data.

6- Acknowledgement

The authors wish to express their deep gratitude for providing Kit Fox field experiment data to Dr. Joseph Chang from George Mason University.

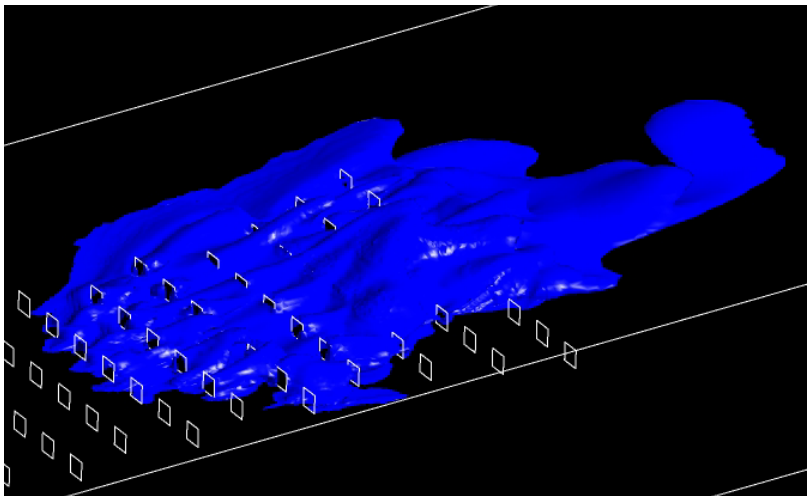

Figure 19. Gas cloud with 150 ppm isosurface concentration, 100s after gas release. Its volume is equal to 2952.4m^3 and its weight is 72kg.

References

1. Markiewicz, M., Models and techniques for health and environmental hazard assessment and management. Center of Excellence Management of Health and Environmental Hazard, Otwock, Swierk (2006).
2. Lees, F. P., Loss prevention in the process industries hazard identification, Assessment and Control, Second edition, Butterworth-Heinemann, (1996).
3. Sklavounos, S. and Rigas, F., "Validation of turbulence models in heavy gas dispersion over obstacles". Journal of Hazardous Materials A108, 9–20 (2004).
4. Hanna, S. R., Hansen, O. R. and Dharmavaram, S., "FLACS CFD air quality model performance evaluation with Kit Fox, MUST, Prairie Grass, and EMU observations". Atmospheric Environment 38, 4675–4687 (2004).
5. Yassin, M.F., Kato, S., Ooka, R., Takahashi, T., Kouno, R., "Field and wind-tunnel study of pollutant dispersion in a built-up area under various meteorological conditions". Journal of Wind Engineering and Industrial Aerodynamics, 93, 361–382 (2005).
6. Kovalets, I.V., Maderich, V.S., "Numerical simulation of interaction of the heavy gas cloud with the atmospheric surface layer". Environmental Fluid Mechanics 6: 313–340 (2006).
7. Mavroidis, I., Andronopoulos, S., Bartzis, J.G., Griffiths, R.F., "Atmospheric dispersion in the presence of a three-dimensional cubical obstacle: Modeling of mean concentration and concentration fluctuations". Atmospheric Environment, 41, 2740–2756 (2007).
8. Wilkening, H., Baraldi, D., "CFD modeling of accidental hydrogen release from pipelines". International Journal of Hydrogen Energy 32 (13), 2206-2215 (2007).
9. Kashi, E., Shahraki, F., Rashtchian, D., Mohebinia, S., "Gas dispersion and explosion over a built-up area with CFD". Amirkabir Journal of Science and Technology, Article in press (2008).
10. Sklavounos, S., Rigas, F., "Simulation of Coyote series trials—Part I: CFD estimation of non-isothermal LNG releases and comparison with box-model predictions". Chemical Engineering Science, 61, 1434–1443 (2006).
11. Hanlin, A. L., Koopman, R. P., Ermak, D. L., "On the application of computational fluid dynamics codes for liquefied natural gas dispersion". Journal of Hazardous Materials 140, 504–517 (2007).
12. Gavelli, F., Bullister, E., Kytomaa, H., "Application of CFD (Fluent) to LNG spills into geometrically complex environments". Journal of Hazardous Materials, Article in press (2008).
13. ANSYS Company, CFX-11 Solver Theory Manual, CFX Ltd., Oxfordshire, pp. 57–96 (2006).
14. McQuaid, J. and Roebuck, B., "Large scale field trials on dense vapor dispersion". Report No. EUR 10029 (EN), pp. 200–204 and 262–267 (1985).
15. Hall, R.C., "Dispersion of releases of hazardous materials in the vicinity of buildings Phase II CFD modelling". Health and Safety Executive (1997).
16. Western Research Institute (WRI), Final Report on the 1995 Kit Fox Project, Vol. I- Experiment Description and Data Processing, and Vol. II- Data Analysis for Enhanced Roughness Tests. WRI, Laramie, Wyoming, 109pp+67pp (1998).
17. Hanna, S. R., Chang, J. C., and Briggs, G. A., "Dense gas dispersion model modifications and evaluations using the Kit Fox Field Observations". Hanna Consultants Report Number P011F, September 15 (1999).
18. Hanna, S. R., Chang, J. C., "Use of the Kit Fox field data to analyze dense gas dispersion modeling issues". Atmospheric Environment 35, 2231-2242 (2001).

19. Carruthers, D., Handbook of Atmospheric Science: Principles and Applications. Blackwell publishing, chap. 10 (2003).
20. Oettl, D., Goulart, A., Degrazia, G. and Anfossi, D., "A new hypothesis on meandering atmospheric flows in low wind speed conditions". Atmospheric Environment Vol 39 (9): 1739-1748 (2005).
21. Shames, I. H., Mechanics of fluids. Second edition, Mc Graw-Hill (1988).
22. Hanna, S. R. and Britter, R. E., Wind flow and vapor cloud dispersion at industrial and urban sites. AIChE Center for Chemical Process Safety, New York, NY (2002).